Resting functional connectivity between the hemispheres in childhood absence epilepsy

X. Bai, PhD
J. Guo, BA
B. Killory, MD
M. Vestal, MD
R. Berman, BA
M. Negishi, PhD
N. Danielson, BA
E.J. Novotny, MD
R.T. Constable, PhD
H. Blumenfeld, MD, PhD

Address correspondence and reprint requests to Dr. Hal Blumenfeld, Yale Departments of Neurology, Neurobiology, and Neurosurgery, 333 Cedar Street, New Haven, CT 06520-8018
hal.blumenfeld@yale.edu

ABSTRACT

Objective: The fundamental mechanisms by which childhood absence epilepsy (CAE) changes neural networks even between seizures remain poorly understood. During seizures, cortical and subcortical networks exhibit bihemspheric synchronous activity based on prior EEG-fMRI studies. Our aim was to investigate whether this abnormal bisynchrony may extend to the interictal period, using a blood oxygen level–dependent (BOLD) resting functional connectivity approach.

Methods: EEG-fMRI data were recorded from 16 patients with CAE and 16 age- and gender-matched controls. Three analyses were performed. 1) Using 16 pairs of seizure-related regions of interest (ROI), we compared the between-hemisphere interictal resting functional connectivity of patients and controls. 2) For regions showing significantly increased interhemispheric connectivity in CAE, we then calculated connectivity to the entire brain. 3) A paired-voxel approach was performed to calculate resting functional connectivity between hemispheres without the constraint of predefined ROIs.

Results: We found significantly increased resting functional connectivity between hemispheres in the lateral orbitofrontal cortex of patients with CAE compared to normal controls. Enhanced between-hemisphere connectivity localized to the lateral orbitofrontal cortex was confirmed by all 3 analysis methods.

Conclusions: Our results demonstrate abnormal increased connectivity between the hemispheres in patients with CAE in seizure-related regions, even when seizures were not occurring. These findings suggest that the lateral orbitofrontal cortex may play an important role in CAE pathophysiology, warranting further investigation. In addition, resting functional connectivity analysis may provide a promising biomarker to improve our understanding of altered brain function in CAE during the interictal period. *Neurology*® 2011;76:1960–1967

GLOSSARY

ANOVA = analysis of variance; **BOLD** = blood oxygen level–dependent; **CAE** = childhood absence epilepsy; **EPI** = echoplanar imaging; **FWE** = familywise error; **MNI** = Montreal Neurological Institute; **ROI** = region of interest; **SWD** = spike-wave discharge.

Childhood absence epilepsy (CAE) is increasingly recognized as a disorder characterized by impaired function both during seizures, and in the interictal period.[1-4] Notably, 3–4 Hz spike-wave discharges (SWD) seen in CAE[5-7] and their associated blood oxygenation level–dependent (BOLD) fMRI changes[8-16] are bilateral and fairly symmetric. Evidence from animal models indicates that this bihemispheric synchrony during SWD is mediated by the corpus callosum.[17,18] We hypothesize that abnormal bihemispheric synchrony persists in the interictal period, and may participate in generating abnormal function, including enhanced bilateral excitability. The possible role of abnormal long-range bilateral synchrony during the interictal period in CAE has not been previously investigated.

The recent development of the resting functional connectivity approach to fMRI has provided a window to observe intrinsic brain activity in health and disease. This method has been used to

Editorial, page 1952

Supplemental data at www.neurology.org

From the Departments of Neurology (X.B., J.G., B.K., M.V., R.B., N.D., E.J.N., H.B.), Diagnostic Radiology (M.N., R.T.C.), Pediatrics (E.J.N.), Neurobiology (H.B.), and Neurosurgery (E.J.N., H.B.), Yale University School of Medicine, New Haven, CT.

Study funding: Supported by NIH R01 NS055829, CTSA UL1 RR0249139 (H.B.), NIH MSTP TG 5T32GM07205 (J.G.), Epilepsy Foundation Fellowship (X.B.), and the Betsy and Jonathan Blattmachr family.

Disclosure: Author disclosures are provided at the end of the article.

Table Clinical information for patients with CAE

Patient	Gender	Age at onset, y	Age at scan, y	Medication prior to scanning[a]	Reported seizure frequency/d at time of onset	No. fixation runs	No. SWD	SWD duration, s
1	Male	13	14	Lamotrigine	None	4	1	4.7
2	Female	11	15	None	240	3	1	2.3
3	Female	8	17	Lamotrigine	10	3	0	—
4	Female	7	8	Levetiracetam	4	4	0	—
5	Male	9	9	Ethosuximide	6	1	0	—
6	Female	5	6	None	10	2	2	9.1, 6.2
7	Female	7	10	Ethosuximide	40	2	0	—
8	Female	9	12	Ethosuximide	20	2	0	—
9	Female	6	8	Lamotrigine	15	2	2	1.0, 0.6
10	Male	5	10	Ethosuximide	12	2	0	—
11	Female	7	11	Ethosuximide	2	2	0	—
12	Female	4	7	None	60	2	2	2.8, 1.1
13	Male	8	14	Lamotrigine, ethosuximide	8	1	2	28.6, 31
14	Female	5	7	Valproate, ethosuximide	5	1	0	—
15	Female	4	6	Ethosuximide	4	1	3	2.1, 2.2, 3.7
16	Female	6	7	Ethosuximide	6	1	8	0.6, 1.4, 1.1, 1.1, 0.4, 1.8, 1.9, 0.9

Abbreviations: CAE = childhood absence epilepsy; SWD = spike-wave discharge.
[a] Patients who were on medication were tested after their medications were temporarily discontinued for up to 48 h prior to scanning.

investigate the impairment of brain networks in patients with temporal lobe epilepsy[19-22] and idiopathic generalized epilepsy[23,24] compared to healthy controls, mainly showing reduced connectivity in patients during the interictal period. In the present study, we hypothesize that the bilateral synchronous nature of CAE pathophysiology leads to abnormally enhanced resting functional connectivity between the 2 hemispheres in specific brain regions involved in the disorder. To examine this hypothesis, we analyzed resting functional connectivity between the hemispheres in children with CAE and controls, using specific regions of interest (ROIs) known to be involved in SWD[8] and a symmetric paired-voxel approach.

METHODS

Subjects. This study was conducted in 16 pediatric patients with CAE (12 female, 13 right-handed, mean ± SD age 10.1 ± 3.5 years) and 16 age- and gender-matched healthy controls (11 female, 15 right-handed, age 10.4 ± 3.5 years). All patients were referred by their pediatric neurologists and fulfilled the following inclusion criteria: 1) clinical diagnosis of CAE based on International League Against Epilepsy criteria[6] and 2) EEG with typical 3- to 4-Hz bilateral spike-wave discharges and normal background activity; and exclusion criteria: no other seizure types, no known structural brain abnormalities, and no other neurologic disorders. Six additional patients underwent EEG-fMRI but were not included because suitable matched controls were not available at the time of analysis. All controls were recruited locally using newspaper, Internet, and flyer postings, and whenever possible we recruited the patients' unaffected siblings or friends from the same demographic group. Clinical information for the 16 patients is summarized in the table. Mean ± SD IQ based on the Wechsler Abbreviated Scale of Intelligence was 105.5 ± 14.9 for patients and 111.4 ± 17.9 for controls. As described previously,[8,15] patients who were on seizure medication were tested after holding their medication for up to 48 hours prior to the scan.

Standard protocol approvals, registrations, and patient consents. Approval was received from the institutional review boards at Yale University School of Medicine (New Haven, CT). The legal guardians of all subjects gave written informed consent, and all subjects gave written or verbal assent prior to participation.

Data acquisition. EEG data were continuously acquired during fMRI from an EEG cap with 32 carbon wire EEG electrodes (in-house) (Neuroscan Inc., Charlotte, NC) and a preamplifier (in-house).[25] EEG data were recorded with a 125-Hz analog low-pass Butterworth filter (in-house) and digitized at 1 kHz with 24-bit data resolution (SynAmps2, Neuroscan Inc.), referenced online to a linked ear reference electrode.

fMRI data were acquired on a 3-T Magnetom Trio scanner (Siemens Medical Systems, Erlangen, Germany) using a standard whole-head coil. Images were recorded with an echoplanar imaging (EPI) sequence with the following parameters: repetition time = 1,550 msec, echo time = 30 msec, flip angle = 80 degrees, and acquisition matrix = 64 × 64. Twenty-five contiguous 6-mm anterior commissure/posterior commissure aligned

axial slices (field of view = 22 cm) were selected to provide coverage of the entire brain. Each functional run consisted of 416 time course image volumes. To avoid head movement, subjects' heads were tightly fixed during the scanning procedure using foam padding. During the resting-state scan, subjects were asked to fixate on a cross with their eyes open. Data runs lasted for 10 minutes and 45 seconds. Up to 4 runs (typically 2 runs) of resting data were obtained per recording session.

EEG analysis. Raw EEG data were processed offline to remove artifact generated by MRI scans, allowing the visualization of the entire EEG trace. Magnetic resonance artifact was subtracted using adaptive noise cancellation software.[25] After artifact removal, EEG data were low-pass filtered with a cutoff frequency of 25 Hz and visually inspected. A trained epilepsy neurologist (H.B.) reviewed the filtered data to identify the onset and duration of any SWD episodes that occurred during scans. All identified SWDs were considered epileptiform abnormalities in the analysis, and no other criteria were used such as SWD duration or clinical behavioral change. In controls, identical EEG setup and cap placement were used, and no EEG abnormalities were observed during a brief screening EEG obtained before entering the scanner. No EEG data were obtained in controls during the scans although the cap remained in place to ensure the experience for patients and controls was identical.

fMRI data processing. Functional image preprocessing was performed using SPM2 (http://www.fil.ion.ucl.ac.uk/spm/) on a MATLAB 7.1 platform (MathWorks, Natick, MA) common to many functional imaging studies. The first 10 images (15.5 seconds) were discarded in each run to avoid transient signal changes before magnetization reached steady-state. The remaining 406 images in each run were spatially realigned to the first image of each functional series to correct for subject motion, using 3-dimensional rigid body transformation with 3 translation and 3 rotation parameters as implemented in the SPM software. Images were spatially normalized into the SPM2 EPI template in MNI space ($4 \times 4 \times 4$ mm resampled voxel size), using a nonlinear 12-parameter affine warping algorithm as implemented in SPM, and spatially smoothed using a 10-mm 3-dimensional Gaussian kernel. For inclusion in the analysis, we required that the transient movement during the analysis period was <1 mm of translation, and <1 degree of rotation.

Preprocessing steps specific to functional connectivity analyses were performed using in-house code written in MATLAB. First, 2 sources of spurious variance were subtracted from the data through linear regression: 1) 6 parameters obtained by rigid body correction of head motion 2) and averaged signal for each slice. Second, data were temporally bandpass filtered ($0.01 < f < 0.08$ Hz) to remove low-frequency drift and to reduce the influence of high-frequency noise. Third, images from -40 s before to $+60$ s after each SWD onset were discarded to avoid the effect of BOLD changes due to SWD. Analysis of SWD-related changes are described elsewhere.[8,15] The first 33 images of the remaining 406 acquisitions in each run were discarded to ensure participants were in the resting state. The remaining images for each patient and matched control were defined as the interictal functional images used in functional connectivity analysis. For each patient and control pair, the timing and number of images used for analysis from each run were matched so that identical timing and number of images were used for patients and controls.

Connectivity analyses based on ROIs. We used a ROI-based correlation method to estimate resting functional connectivity between the hemispheres. All ROIs were 20-mm-diameter spheres and were selected based on our recent study, which showed peak fMRI increases related to SWD in specific regions described below.[8] These areas are also highly consistent with activations reported in other studies.[9-11,13] Sixteen total pairs of left and right ROIs were constructed using MARSBAR (http://marsbar.sourceforge.net/) as follows (ROI centers in MNI coordinates) (figure e-1 on the *Neurology*® Web site at www.neurology.org): orbitofrontal cortex 1 (medial orbitofrontal) ($\pm 10, 42, -17$) and 2 (lateral orbitofrontal) ($\pm 44, 37, -9$); medial frontal cortex 1 ($\pm 10, 58, -10$) and 2 ($\pm 10, 41, 8$); lateral frontal cortex 1 ($\pm 47, 26, 28$) and 2 ($\pm 34, 0, 58$); cingulum ($\pm 10, -4, 44$); precuneus 1 ($\pm 10, -58, 18$) and 2 ($\pm 10, -54, 38$); occipital ($\pm 10, -85, 4$); lateral parietal cortex ($\pm 48, -62, 36$); medial temporal ($\pm 22, -1, -28$); lateral temporal cortex ($\pm 62, -41, -20$); thalamus ($\pm 10, -18, 8$); basal ganglia ($\pm 14, 7, 2$); and cerebellum ($\pm 49, -62, -28$).

To prepare data for ROI-based analyses, we first calculated correlation maps between fMRI signal in each ROI and the whole brain, and converted these into z score maps. To accomplish this, for each individual subject the mean time course was extracted from all voxels within the seed ROI. A correlation map for this seed ROI was then produced by computing the Pearson correlation coefficient r between the mean time course and the time course from all other voxels. Subsequently, this correlation map was converted to a z score map by Fisher z transform equation $z(r) = 0.5\ln[(1 + r)/(1 - r)]$.[26] To normalize for differences in number of images, each z score was divided by the square root of variance, calculated as $1/\sqrt{(n - 3)}$, where n is the degrees of freedom defined as the number of image acquisitions within each run. For subjects with multiple runs, the resulting z score map was computed by averaging z score maps across individual runs. Since there were 32 ROIs (16 in each hemisphere), this resulted in a total of 32 individual z score maps obtained for each subject.

We then performed 2 types of ROI-based analysis: 1) connectivity between each ROI and its corresponding ROI in the contralateral hemisphere and 2) connectivity between each ROI and all other brain regions. For the first analysis, we calculated the between-hemisphere connectivity as the average z score in the ROI contralateral to each seed ROI (32 values total, or 16 pairs between the hemispheres) for each subject. For group statistical analyses, we then performed one-way analysis of variance (ANOVA) followed by Tukey HSD method for post hoc pairwise comparisons (significance threshold $p < 0.05$) to assess the group differences in patients vs controls for each ROI (total 32 comparisons).

Next, for regions such as orbitofrontal cortex, which showed significant differences in between-hemisphere connectivity in the ANOVA, we constructed t maps to examine connectivity to all other brain regions. To accomplish this, the individual z score maps of each group (patients and controls) for each seed ROI were entered into a second-level, one-sample t test ($p < 0.01$, familywise error [FWE] corrected, cluster extent threshold = 3 voxels) in SPM2. Analysis was confined to the gray matter by applying a standard gray matter mask from MarsBaR (http://marsbar.sourceforge.net/) to all z score maps.

Connectivity analysis using subthreshold paired-voxel approach. The hypothesis-based analyses above were used to determine if significant differences existed between patients and controls in specific ROIs. However, as an exploratory analysis, we were interested in determining whether even greater differences might exist in regions not considered by the predefined ROIs. We therefore used a paired-voxel correlation approach to assess group difference in patients vs controls for the entire brain.

Figure 1 Lateral orbitofrontal cortex (OF2) shows significant increase in between-hemisphere connectivity in childhood absence epilepsy

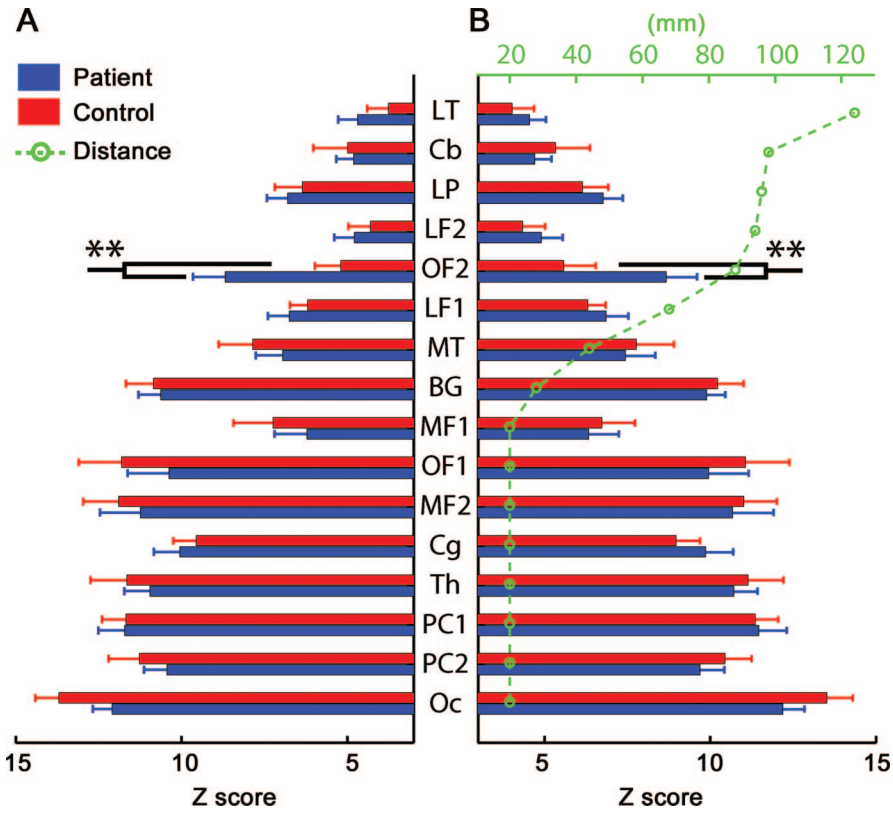

Statistical comparisons of between-hemisphere resting-state functional connectivity in 16 patients vs 16 matched controls. (A) Seed region of interest (ROI) in the left hemisphere and mean connectivity in the corresponding right hemisphere ROI. (B) Seed ROI in the right hemisphere and mean connectivity in the corresponding left hemisphere ROI. Values are mean connectivity (*z* score), and error bars are SD. **Significant differences between patients and controls using one-way analysis of variance with Tukey method for post hoc pairwise comparisons, (A) $F = 8.73$, $p = 0.006$ (for OF2); (B) $F = 5.59$, $p = 0.025$ (for OF2). Green circles and the green scale represent the interhemispheric distance between each pair of ROIs. BG = basal ganglia; Cb = cerebellum; Cg = cingulum; LF1 = lateral frontal 1; LF2 = lateral frontal 2; LP = lateral parietal; LT = lateral temporal; MF1 = medial frontal 1; MF2 = medial frontal 2; MT = medial temporal; Oc = occipital; OF1 = orbitofrontal 1 (medial orbitofrontal); OF2 = orbitofrontal 2 (lateral orbitofrontal); PC1 = precuneus 1; PC2 = precuneus 2; Th = thalamus.

For each subject, a Pearson correlation was computed between the time courses for pairs of symmetrically located voxels, i.e., 2 voxels with matching coordinates in the left and right hemispheres in Montreal Neurological Institute (MNI) space (opposite x, same y, and z). The resulting correlation map was converted to a *z* score map using the same method described above. Finally, all individual *z* score maps for patients and controls were entered into a second-level, 2-sample *t* test. Because the statistical power of this second-level analysis for the entire brain is less than the hypothesis-based approach, and because we were only interested in detecting possible group differences that were greater than those seen in the predefined ROIs, we used an uncorrected height threshold of $p < 0.005$ (cluster extent threshold = 3 voxels) in SPM2 to detect any potential subthreshold differences.

RESULTS We found significantly increased resting functional connectivity between the left and right lateral orbitofrontal cortex in patients with CAE compared to matched controls. Using an ROI-based approach, there was a general trend for increased between-hemisphere connectivity in both patients and controls for structures located closest to the midline corpus callosum (figure 1, green inset). Despite the fact that the lateral orbitofrontal cortex is located relatively far from the midline, patients with CAE demonstrated significantly higher between-hemisphere connectivity in this region than controls (figure 1, OF2). Furthermore, the lateral orbitofrontal cortex was the only region with a significant difference in between-hemisphere connectivity in patients with CAE vs controls, with no significant differences observed in the other 15 ROIs examined by ANOVA. We did not find a significant correlation between the individual connectivity of lateral orbitofrontal cortex (OF2) and seizure severity (SWD/minute scan time), at least with the limited sample size of the present study.

We next examined resting functional connectivity between the lateral orbitofrontal cortex

Figure 2 Lateral orbitofrontal cortex in patients with childhood absence epilepsy shows increased connectivity to the contralateral homologous region

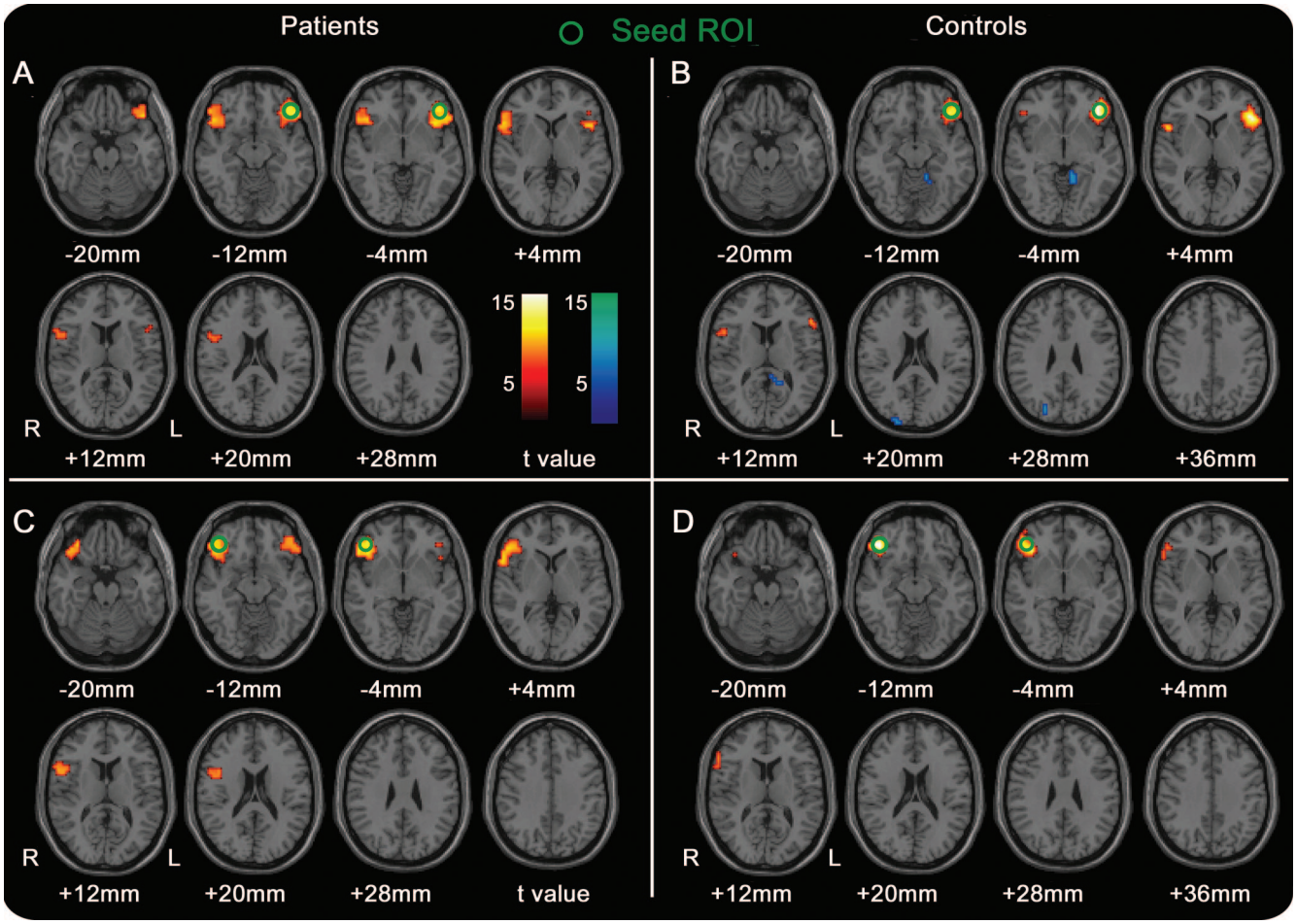

(A) Patients with left seed region of interest (ROI). (B) Controls with left seed ROI. (C) Patients with right seed ROI. (D) Controls with right seed ROI. Statistical maps of resting-state functional connectivity using the lateral orbitofrontal ROI (OF2) were created for each group using a second-level, one-sample *t* test with threshold $p = 0.01$, familywise error-corrected, and extent threshold $k = 3$ voxels (voxel dimensions $4 \times 4 \times 4$ mm). Positive and negative *t* values are warm and cool colors, respectively. The green circle represents the seed ROI.

(OF2) and the entire brain using a one-sample *t* test (threshold $p < 0.01$, FWE-corrected) to determine if other brain regions are involved. Patients with CAE exhibited significant connectivity mainly to the contralateral lateral orbitofrontal cortex, using either the right or left OF2 as the seed region (figure 2, A and C); we did not observe similar connectivity between OF2 and other brain regions. Control subjects showed less contralateral orbitofrontal connectivity with the left seed region (figure 2B) compared to patients, and no significant contralateral connectivity with the right seed region (figure 2D). Control subjects also showed a few small areas of negative connectivity in the medial parietal and occipital cortex with the left seed region (figure 2B).

Using an additional approach to determine regions of highest between-hemisphere connectivity in patients with CAE vs controls, we performed an exploratory subthreshold analysis of all left–right hemisphere voxel pairs (figure 3). The goal was to determine whether greater differences might exist between patients and controls in regions outside the predefined ROIs. As expected, many regions showed strong connectivity between the hemispheres in both groups (data not shown). However, no regions showed greater connectivity differences in patients vs controls than the lateral orbital frontal cortex. Thus, subthreshold analysis again found the greatest increase in between-hemisphere resting connectivity in patients with CAE vs controls was in the lateral orbitofrontal cortex (figure 3), overlapping with the predefined lateral orbitofrontal ROI. Several regions of reduced between-hemisphere subthreshold connectivity were also observed (figure 3) which were not captured by the predetermined ROIs (figure e-1). However, no additional regions of increased between-hemisphere connectivity were observed.

Figure 3 **Whole brain subthreshold analysis confirms that lateral orbitofrontal cortex shows largest increase in between-hemisphere connectivity in childhood absence epilepsy (CAE)**

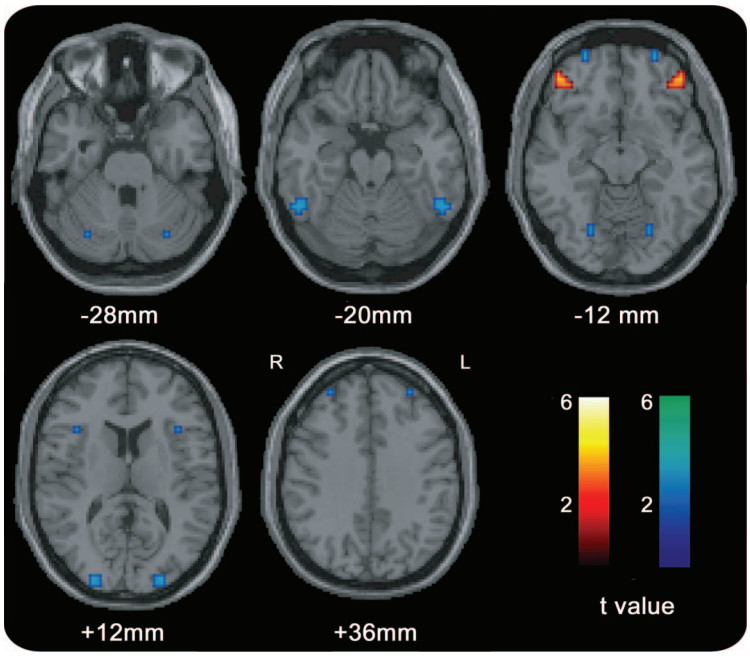

Statistical maps of resting-state functional connectivity between hemispheres using a paired-voxel method. Group analysis of patients with CAE vs controls using 2-sample *t* test, threshold $p = 0.005$, uncorrected, and extent threshold $k = 3$ voxels (voxel dimensions $4 \times 4 \times 4$ mm). Warm colors indicate between-hemisphere connectivity in patients > controls, and cold colors patients < controls.

DISCUSSION Using resting functional connectivity to analyze fMRI data, we investigated the properties of bilateral brain networks in patients with CAE during the interictal period. We observed that the lateral orbital frontal cortex showed significantly increased resting functional connectivity between hemispheres in CAE. These findings may have important implications for understanding abnormal network activity in this disorder. While CAE is considered a "generalized" form of epilepsy, recent evidence suggests that in reality SWD emerge from focal abnormal circuits in the bilateral hemispheres.[27,28] The present findings provide further evidence for focal bilateral network abnormalities in CAE which may contribute to abnormal synchrony and excitability during the interictal period.

Spatial patterns of connectivity between and within hemispheres have been found in many resting state studies of healthy controls,[29-31] revealing consistent regions with similar functionality such as memory, motor, sensory, visual, language, and cognition. At rest, these areas are correlated in their low-frequency spontaneous BOLD activity. Previous studies in depression, Alzheimer disease, attention-deficit/hyperactivity disorder, and schizophrenia have indicated that altered brain functions can be assessed by comparing spatial patterns of resting functional connectivity between patients and controls.[32] Recent EEG-fMRI studies of CAE and related forms of generalized epilepsy demonstrate significant BOLD signal changes during seizures in a complex network of cortical and subcortical areas.[8,10,11,13,16]

Interestingly, CAE characteristically displays widespread, bilaterally synchronous SWD on EEG recordings[5-7,33] and bilaterally symmetric BOLD fMRI changes during seizures.[8-10,16] The present findings support the notion that abnormal bilateral network synchrony occurs during the interictal period as well, operating at a slower time scale, and preferentially involving the lateral orbitofrontal cortices. While most prior studies of brain disorders showed decreased connectivity,[32] it is reasonable to expect increased between-hemisphere connectivity in regions involved in CAE because it emerges from bilateral abnormal enhanced excitability. One could speculate that the abnormally enhanced interhemispheric connectivity we observed could represent a preseizure or subthreshold excitatory phenomenon not detectable on scalp EEG.

A resting functional connectivity approach offers several advantages in studying interictal changes in CAE. The relatively slow time scale of neurometabolic and neurovascular events measures by fMRI resting connectivity provides a window into disease pathophysiology over the longer time scale of the interictal period. Furthermore, in contrast to EEG, fMRI allows for detection of signals from small regions such as the orbitofrontal cortex that are not close to the skull surface. Of note, other neuroimaging techniques, including fluoro-2-deoxy-D-glucose PET,[34,35] magnetic resonance spectroscopy,[36] and voxel-based morphometry in MRI,[37] have also been useful in investigating interictal changes in idiopathic generalized epilepsy. Like these other methods, the resting functional connectivity could potentially serve as a useful biomarker for CAE during the interictal period, with the advantage of detecting abnormal network function. The differences between patients vs controls in the present sample were not sufficiently strong to classify individual subjects reliably; however, further studies with larger samples and under different treatment conditions may yield important insights.

Although our results do not determine the precise role of orbitofrontal cortex in the CAE network, other recent studies[5,37] have also suggested that the orbitofrontal area may play a key role in CAE. Voxel-based morphometry has shown significantly smaller gray matter volumes in the left orbitofrontal cortex in children with CAE compared to healthy controls.[37] High-density scalp EEG and equivalent dipole methods suggest that orbitofrontal and dorsolateral frontal

cortex are active at absence seizure onset.[5] However, morphometric analysis has also shown anatomic abnormalities in other areas such as the temporal lobes,[37] thalamus, and subcallosal gyrus,[12,38] where we did not observe abnormal interhemispheric connectivity in CAE.

In contrast to our results with CAE, previous studies of temporal lobe epilepsy have shown consistently reduced functional connectivity in the interictal areas responsible for cognition, language, and memory.[19-22] These findings suggest that like other chronic brain disorders,[32] impaired cognitive function in epilepsy may be associated with decreased basal interactions between the affected regions. The present study did not investigate cognitive or behavioral impairment in CAE. However, altered function of the orbitofrontal cortex may affect essential behaviors such as arousal, motivation, and impulsivity.[37] In addition, interictal deficits in attention are a major feature of CAE,[4,39-41] and relating abnormal decreases in between- and within-hemisphere connectivity to abnormal attention function in CAE is the subject of another ongoing investigation by our group.[39]

Our findings indicate that some areas within the CAE-related network are abnormally active not only during the ictal period, but also during the interictal period. The abnormal increased connectivity between the lateral orbitofrontal cortex in the 2 hemispheres could play an important role in the pathophysiology of CAE and behavioral changes in patients, and warrants additional investigation. Furthermore, resting functional connectivity analysis may prove to be a promising biomarker of CAE during the interictal period and increase our understanding of the fundamental network dysfunction in this form of epilepsy. These findings have important functional and theoretical implications for understanding the mechanism of CAE.

AUTHOR CONTRIBUTIONS

Xiaoxiao Bai performed statistical analysis and wrote the manuscript. Jennifer Guo, Brendan Killory, Matthew Vestal, Rachel Berman, and Michiro Negishi designed the study and acquired the data. Nathan Danielson participated in data analysis. Edward J. Novotny, R. Todd Constable, and Hal Blumenfeld designed the study and helped write the manuscript.

ACKNOWLEDGMENT

The authors thank the following clinicians who referred patients for the study: W. Brown, R. Duckrow, J. Gaitanis, J. Gibbons, R. Gupta, L. Kan, A. Mower, G. Miller, P. Overby, M. Scher, Y. Sogawa, R. Smith, and E. Wylie. They also thank Michelle Hampson and Jennifer Roth for discussion about the methods.

DISCLOSURE

Dr. Bai received a postdoctoral research training fellowship from the Epilepsy Foundation. J. Guo has received research support from the NIH. Dr. Killory and Dr. Vestal report no disclosures. R. Berman has received research support from the NIH. Dr. Negishi has received research support from the NIH. N. Danielson has received research support from the NIH. Dr. Novotny has served on the speakers' bureau for and received speaker honoraria from UCB and has received research support from Johnson & Johnson, NIH/NINDS, and University of Washington School of Medicine/Seattle Children's Hospital. Dr. Constable serves as Deputy Editor of *Magnetic Resonance in Medicine* and has received research support from the NIH and the Manton Foundation Project. Dr. Blumenfeld receives research support from the NIH, CTSA, and the Betsy and Jonathan Blattmachr family.

Received September 2, 2010. Accepted in final form December 3, 2010.

REFERENCES

1. Andermann F. What is a generalized epilepsy? In: Hirsch E, Andermann F, Chauvel P, Engel J, Lopes da Silva F, Luders H, eds. Generalized Seizures: From Clinical Phenomenology to Underlying Systems and Networks. Montrouge: John Libbey Eurotext; 2006:23–32.
2. Blumenfeld H. Consciousness and epilepsy: why are patients with absence seizures absent? Prog Brain Res 2005; 150:271–286.
3. Hughes JR. Absence seizures: a review of recent reports with new concepts. Epilepsy Behav 2009;15:404–412.
4. Glauser TA, Cnaan A, Shinnar S, et al. Ethosuximide, valproic acid, and lamotrigine in childhood absence epilepsy. N Engl J Med 2010;362:790–799.
5. Holmes M, Brown M, Tucker D. Are "generalized" seizures truly generalized? Evidence of localized mesial frontal and frontopolar discharges in absence epilepsia. Epilepsia 2004;12:1568–1579.
6. Commission on Classification and Terminology of the International League Against Epilepsy. Proposal for revised classification of epilepsies and epileptic syndromes. Epilepsia 1989;30:389–399.
7. Sadleir L, Farrell K, Smith S, Connolly M, Scheffer I. Electroclinical features of absence seizures in childhood absence epilepsy. Neurology 2006;67:413–418.
8. Bai X, Vestal M, Berman R, et al. Dynamic time course of typical childhood absence seizures: EEG, behavior, and functional magnetic resonance imaging. J Neurosci 2010; 30:5884–5893.
9. Laufs H, Lengler U, Hamandi K, Kleinschmidt A, Krakow K. Linking generalized spike-and-wave discharges and resting state brain activity by using EEG/fMRI in a patient with absence seizures. Epilepsia 2006;47:444–448.
10. Salek-Haddadi A, Lemieux L, Merschhemke M, Friston KJ, Duncan JS, Fish DR. Functional magnetic resonance imaging of human absence seizures. Ann Neurol 2003;53: 663–667.
11. Aghakhani Y, Bagshaw AP, Benar CG, et al. fMRI activation during spike- and wave-discharges in idiopathic generalized epilepsy. Brain 2003;127:1127–1144.
12. Chan C, Briellmann R, Pell G, Scheffer I, Abbott D, Jackson G. Thalamic atrophy in childhood absence epilepsy. Epilepsia 2006;47:399–405.
13. Gotman J, Grova C, Bagshaw A, Kobayshi E, Aghakhani Y, Dubeau F. Generalized epileptic discharges show thalamocortical activation and suspension of the default state of the brain. Proc Natl Acad Sci USA 2005;102: 15236–15240.
14. Hamandi K, Salek-Haddadi A, Laufs H, et al. EEG-fMRI of idiopathic and secondarily generalized epilepsies. Neuroimage 2006;31:1700–1710.

15. Berman R, Negishi M, Vestal M, et al. EEG, fMRI, and behavior in typical childhood absence seizures. Epilepsia 2010;51:2011–2022.
16. Moeller F, Siebner HR, Wolff S, et al. Changes in activity of striato-thalamo-cortical network precede generalized spike wave discharges. Neuroimage 2008;39:1839–1849.
17. Musgrave J, Gloor P. The role of the corpus callosum in bilateral interhemispheric synchrony of spike and wave discharge in feline generalized penicillin epilepsy. Epilepsia 1980;21:369–378.
18. Vergnes M, Marescaux C, Lannes B, Depaulis A, Micheletti G, Warter J. Interhemispheric desynchronization of spontaneous spike-wave discharges by corpus callosum transection in rats with petit mal-like epilepsy. Epilepsy Res 1989;4:8–13.
19. Waites AB, Briellmann RS, Saling MM, Abbott DF, Jackson GD. Functional connectivity networks are disrupted in left temporal lobe epilepsy. Ann Neurol 2006;59:333–343.
20. Bettus G, Guedj E, Joyeux F, et al. Decreased basal fMRI functional connectivity in epileptogenic networks and contralateral compensatory mechanisms. Hum Brain Mapp 2009;30:1580–1591.
21. Liao W, Zhang Z, Pan Z, et al. Altered functional connectivity and small-world in mesial temporal lobe epilepsy. PLoS ONE 2010;5:e8525.
22. Zhang Z, Lu G, Zhong Y, et al. Impaired perceptual networks in temporal lobe epilepsy revealed by resting fMRI. J Neurol 2009;256:1705–1713.
23. Lui S, Ouyang L, Chen Q, et al. Differential interictal activity of the precuneus/posterior cingulate cortex revealed by resting state functional MRI at 3T in generalized vs. partial seizure. J Magn Reson Imaging 2008;27:1214–1220.
24. Luo C, Li Q, Lai Y, et al. Altered functional connectivity in default mode network in absence epilepsy: a resting-state fMRI study. Hum Brain Mapp Epub 2010.
25. Negishi M, Abildgaard M, Laufer I, Nixon T, Constable R. An EEG (electroencephalogram) recording system with carbon wire electrodes for simultaneous EEG-fMRI (functional magnetic resonance imaging) recording. J Neurosci Methods 2008;173:99–107.
26. Jenkins G, Watts D. Spectral Analysis and its Applications. San Francisco, CA: Holden-Day; 1968.
27. Blumenfeld H. Cellular and network mechanisms of spike-wave seizures. Epilepsia 2005;46:21–33.
28. Meeren H, van Luijtelaar G, Lopes da Silva F, Coenen A. Evolving concepts on the pathophysiology of absence seizures: the cortical focus theory. Arch Neurol 2005;62:371–376.
29. Biswal BB, Mennes M, Zuob X-N, et al. Toward discovery science of human brain function. Proc Natl Acad Sci USA 2010;107:4734–4739.
30. Fox MD, Raichle ME. Spontaneous fluctuations in brain activity observed with functional magnetic resonance imaging. Nat Rev Neurosci 2007;8:700–711.
31. Fransson P, Skiold B, Horsch S, et al. Resting-state networks in the infant brain. Proc Natl Acad Sci USA 2007;104:15531–15536.
32. Auer DP. Spontaneous low-frequency blood oxygenation level-dependent fluctuations and functional connectivity analysis of the 'resting' brain. Magn Reson Imaging 2008;26:1055–1064.
33. Yeni SN, Kabasakal L, Yalcinkaya C, Nisli C, Dervent A. Ictal and interictal SPECT findings in childhood absence epilepsy. Seizure 2000;9:265–269.
34. Hikima A, Mochizuki H, Oriuchi N, Endo K, Morikawa A. Semiquantitative analysis of interictal glucose metabolism between generalized epilepsy and localization related epilepsy. Ann Nucl Med 2004;18:579–584.
35. Ciumas C, Wahlin T, Espino C, Savic I. The dopamine system in idiopathic generalized epilepsies: identification of syndrome-related changes. Neuroimage 2010;51:606–615.
36. Helms G, Ciumas C, Kyaga S, Savic I. Increased thalamus levels of glutamate and glutamine (Glx) in patients with idiopathic generalised epilepsy. J Neurol Neurosurg Psychiatry 2006;77:489–494.
37. Caplan R, Levitt J, Siddarth P, et al. Frontal and temporal volumes in childhood absence epilepsy. Epilepsia 2009;50:2466–2472.
38. Betting L, Mory S, Lopes-Cendes I, et al. MRI volumetry shows increased anterior thalamic volumes in patients with absence seizures. Epilepsy Behav 2006;8:575–580.
39. Killory BD, Bai X, Negishi M, et al. Impaired attention and network connectivity in childhood absence epilepsy. Neuroimage Epub 2011 Mar 21.
40. Vega C, Vestal M, DeSalvo M, et al. Differentiation of attention-related problems in childhood absence epilepsy. Epilepsy Behav 2010;19:82–85.
41. Caplan R, Siddarth P, Stahl L, et al. Childhood absence epilepsy: behavioral, cognitive, and linguistic comorbidities. Epilepsia 2008;49:1838–1846.